Materials Science and Engineering C 62 (2016) 391–397

Contents lists available at ScienceDirect

Materials Science and Engineering C

journal homepage: www.elsevier.com/locate/msec

# Capillary microfluidics-derived doxorubicin-containing human serum albumin microbeads for transarterial chemoembolization of hepatic cancer

Min-Kyoung Kim [a,1], Min A. Kim [b,1], Ratchapol Jenjob [a], Don-Haeng Lee [a,b], Su-Geun Yang [a,*]

[a] Department of New Drug Development, School of Medicine, Inha University, Incheon 400-712, Republic of Korea
[b] Division of Gastroenterology & Hepatology, Inha University Hospital, Incheon 400-712, Republic of Korea

ARTICLE INFO

*Article history:*
Received 23 July 2015
Received in revised form 18 January 2016
Accepted 27 January 2016
Available online 29 January 2016

*Keywords:*
Hepatocellular carcinoma
Transarterial chemoembolization
Doxorubicin
Capillary microfluidics
Albumin microparticles

ABSTRACT

In this study, we prepared doxorubicin (DOXO)-loaded albumin microbeads (DOXO-MBs) using a capillary microfluidic device for transarterial chemoembolization of hepatic cancer. Albumin droplets were fabricated using the capillary microfluidic device and solidified by addition of glutaraldehyde. The acquired DOXO-MBs were homogeneous and the size was adjustable from 183.2 ± 12.2 μm to 351.5 ± 7.9 μm by changing the flow rate of fluidic solutions. The loading amount of DOXO was 9.7 ± 1.5 mg/g, and over 15.7% of DOXO was released over one month in pH 7.2 buffer. Intra-portal injection of DOXO-MBs on normal liver of rats proved microbeads efficiently embolized hepatic vessels. Hepatic lobes, recovered 24 days after intra-portal injection, showed that the DOXO-MBs remained in hepatic vessels and released DOXO to surrounding hepatic tissues. In the hepatic tumor xenograft mouse model, DOXO-MBs inhibited tumor growth more efficiently than intravenous (I.V.) injection of free DOXO ($p < 0.01$).



## 1. Introduction

Hepatocellular carcinoma (HCC) ranks as the fourth most common cancer death in the world. In 2008, newly 748,000 cases of HCC were diagnosed and approximately 696,000 people died from HCC in worldwide [1,2]. Age-standardized incidence rates per 100,000 range from 2.1 North America to 80 in China [3].

HCC primarily progresses from chronic liver inflammation and consequential cirrhosis. Up to 90% of HCC has a cirrhotic background. Thus, most hepatic malignancies are unresectable due to hepatic dysfunction. On early stage of HCC, a curative therapy (i.e., surgical resection) is conceivable, but half of the patients after surgical resection undergo recurrence within 2 years [4,5]. Recently-approved drugs for HCC do not seem to be effective in advanced cases [6]. Consequently alternative interventional therapies have been tried for management of unresectable HCC [7–10]. Among them, transcatheter arterial chemoembolization (TACE) showed the promising clinical results on survival rate [11,12].

TACE is a combination therapy of arterial obstruction and local chemotherapy. After the introduction of Lipiodol as a drug carrier in the early 1980s, TACE has become one of the standard treatments for HCC [13]. However, instability of Lipiodol emulsion always caused great concern about the therapeutic efficacy. Johnson et al. reported that no difference was detected in pharmacokinetic parameters or toxicity between intra-arterial injection of doxorubicin with Lipiodol and intravenous doxorubicin [14].

Recently cancer-drug loaded microbeads were approved for TACE and displayed promising clinical outcomes [11,15]. The injected microbeads occlude the tumor's blood supply and release doxorubicin for extended periods [16,17]. Currently two types of drug-eluting beads are available in the market: DC bead® (Biocompatibles, London, England) and Quadrasphere™ microbeads (South Jordan, UT, USA) [16,18].

In this study, we applied human serum albumin (HSA) for a biocompatible and biodegradable drug carrier and fabricated the doxorubicin (DOXO)-loaded albumin microbeads (DOXO-MBs) using a capillary microfluidic system. For microbead-based TACE, it is important to control the size, shape and properties of beads [19]. So we applied capillary microfluidics to acquire the drug-loaded and homogeneous microbeads. Capillary microfluidics is the most powerful approach for obtaining highly monodispersed microdroplets. David A. Weitz and his group reported various capillary fluidic systems that can make diverse types of droplets (single, double and multiple emulsion droplets) [20], but their applications were confined to oily droplet formation. Nowadays more versatile applications have been developed. Solid microspheres, alginate based-microfiber or living cell-encapsulating beads can be fabricated using capillary fluidic devices.

* Corresponding author at: Department of New Drug Development, School of Medicine, Inha University, 8F A-dong, Jeongseok Bldg., 366, Seohaedaero, Incheon 400-712, Republic of Korea.
*E-mail address:* Sugeun.Yang@Inha.ac.kr (S.-G. Yang).
[1] Both authors equally contributed to this work.

http://dx.doi.org/10.1016/j.msec.2016.01.073
0928-4931/

The vascular embolization of DOXO-MBs was observed in rat liver after intra-portal vein administration using an in vivo optical imaging system and tissue histology. In vivo antitumor effect of the microbeads was evaluated using a human liver tumor xenograft model.

## 2. Experimental

### 2.1. Materials

Human serum albumin (HSA) was purchased from Green Cross Co. (Seoul, South Korea). Glutaraldehyde, Tween 80 and Span 80 were purchased from Sigma Chemical Co. (St. Louis, MO, USA). Doxorubicin HCl (DOXO) was kindly provided by Boryung Pharmaceutical Co. (Seoul, South Korea). Capillary glass tubes were purchased from World Precision Instruments (Sarasota, FL, USA), square glass tubes were purchased from Vitrocom Inc. (Mountain Lakes, NJ, USA), and glass slides were purchased from Paul Marienfeld Gmbh & Co. (Lauda-Konigshofen, Germany). Epoxy glue was purchased from Huntsman Advanced Materials (Basel, Switzerland). Medium chain triglyceride (MCT) oil (Labrafac CC®) was purchased from Gattafosse (Cedex, France). All other reagents were of analytical grade and used without further purification.

### 2.2. Preparation of the DOXO-MBs

A simple microfluidic device was constructed using borosilicate glass capillary tubes on glass slides as previously reported [20–24]. The inner dimension of the square capillary was 1.0 m and the cylindrical capillary had an inner diameter of 0.58 mm and an outer diameter of 1.0 mm.

The cylindrical capillary glass tube was tapered by heating with a torch and hand pulling. The tip of the tapered cylindrical tube was flattened using salt paper and measured using a microscope; tips with a diameter ranging from 200 to 250 μm were selected. The tapered cylindrical tube was inserted into the square tube coaxially, by matching the outer diameter of the cylindrical tube to the inner dimension of the square one. Syringes were fixed on both the ends of the square tube using epoxy glue and covered well with glue to prevent any leakage. Two immiscible liquids were supplied separately to the microfluidic device through polyethylene tubing attached with syringes driven by syringe pumps (KD 200, KD Scientific Inc., Holliston, MA). The schematic illustration of the microfluidic device is shown in Fig. 1. The oil phase consisted of MCT oil with 1% (volume/volume; v/v) Span 80 and 75 μl of glutaraldehyde, and the aqueous phase consisted of 20% (v/v) HSA solution with 0.2% (weight/volume; w/v) DOXO and 3% (v/v) Tween 80. The collection phase consisted of 200 ml MCT oil. These two immiscible fluids were introduced by two independent syringe pumps for the dispersed (aqueous phase) and continuous phase (oil phase) at flow rates of 3 ml/h and 10 ml/h, respectively. The liquid droplets were formed at the end of the ~250 μm capillary tip and collected simultaneously into the collection phase for 10 min. The collection phase was continuously mixed by stirring with magnetic bar at 80 rpm, and the glutaraldehyde was neutralized by 100 ml of 5% sodium bisulfate solution. Overall preparation was performed at room temperature (20 ± 2 °C). The microbeads were then washed five times with double distilled water (DDW) and stored at 4 °C for further studies.

### 2.3. Characterization of DOXO-MBs

The morphology of DOXO-MBs was characterized by microscopy (DM2500, Leica, Wetzlar, Germany) and scanning electron microscopy (SEM) (SNE-4000M, SEC, Suwon, South Korea). The DOXO-MBs were imbedded on a paraffin block and cross-sectioned for SEM analysis. Inner structure of DOXO-MBs was observed by SEM.

The content of DOXO was determined by dissolving the microbeads (25 mg) in 0.1 N HCl containing 10% pepsin, followed by UV–visible spectrophotometry (Hitachi U-2900, Hitachi, Japan) at 480 nm with an appropriate dilution.

### 2.4. In vitro release studies

In vitro release of DOXO-MBs was estimated in release medium. Briefly, 500 mg of DOXO-MBs were placed in a 50-ml glass bottle with

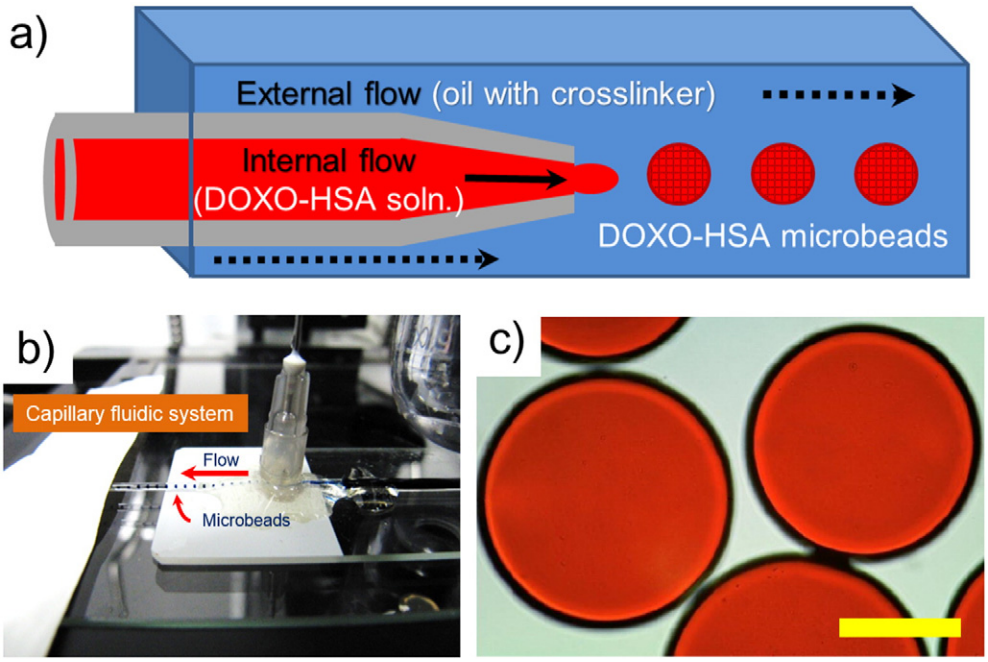


**Fig. 1.** Capillary microfluidic system for fabrication of DOXO-containing microbeads. (a) Schematic illustration of a capillary microfluidic system used in this study, inner fluid: aqueous DOXO-albumin solution, outer fluid: medium chain triglyceride with crosslinking agent. (b) Photo-image of capillary microfluidic system, microbeads stained with methylene blue are formed at the end of inner fluidic capillary and flow to collector. (c) Microscopic observation of DOXO-containing microspheres (DOXO-MBs), scale bar represents 100 μm in length.

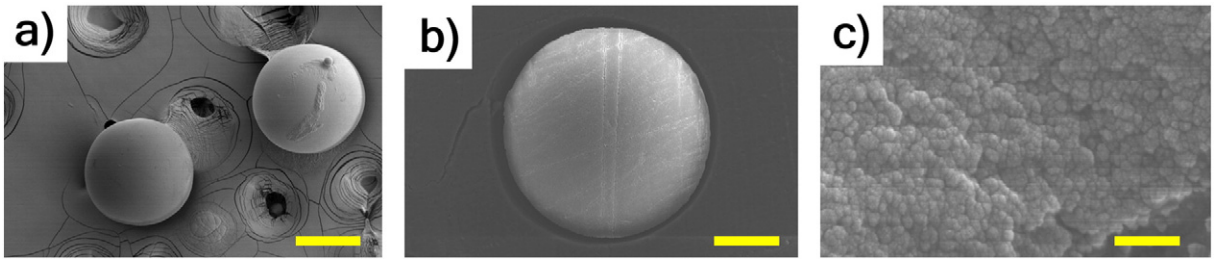


**Fig. 2.** Solid formation of albumin microbeads with outer fluidic aldehyde crosslinking (a) SEM observation of DOXO-MBs, fabricated by capillary microfluidics. Scale bar represents 200 μm. (b) SEM observation of cross-sectioned DOXO-MBs at ×1000 magnification. Scale bar represents 100 μm. (c) SEM observation of cross-sectioned DOXO-MBs. Solid and rigid formation of microbeads was confirmed via SEM analysis. Scale bar represents 200 nm.

a plastic cap, and then 30 ml buffer were added. The bottle was kept in a water bath at 37 °C in dark with stirring at 50 rpm [25]. At predetermined time intervals (for 30 days), 0.3 ml of samples were collected and replaced with the same volume of buffer. The collected samples were analyzed for doxorubicin content by fluorescent spectrophotometry (F-7000, Hitachi, Japan) with appropriate dilution.

### 2.5. Portal vein injection of DOXO-MBs

Male Sprague–Dawley rats (250–300 g, Orient Bio Co., Korea) were selected for the study. All animal care and procedures were conducted according to the Guiding Principles in the use of animals established by Inha University. The rats were anesthetized via isoflurane inhalation, secured on the dissection plate and then the abdomen was opened for injection. Two hundred microliters of DOXO-MBs (around 100 μm in size) was injected into the portal vein after dilution with 1 ml of normal saline. After injection of the microbeads, the needle was kept in the portal vein for 5 min with slight pressure using cotton soaked in ethanol. Then liver was carefully excised from the rats and washed several times with PBS solution. Fluorescence images of the recovered liver were obtained using a Maestro in-vivo fluorescence imaging system (CRI, Woburn, MA, USA) in the cube acquisition mode. The pure autofluorescence spectra of DOXO and DOXO-MBs were manually selected from the spectral image using DOXO solution to select appropriate regions.

Liver was recovered 24 days after portal vein injection, placed in a mold filled with Tissue-Tek® O.C.T. Compound and dipped in $N_2$ solution; sections were prepared using a cryotom (Shandon Cryotome® SME, Fisher Scientific, Leicestershire, UK). The prepared sections were observed using an up-light fluorescence microscope (DM 2500®, Leica, Wetzlar, Germany).

### 2.6. In vivo antitumor activities of DOXO-MBs

In this study, we used hepatic cancer xenograft mouse model to prove the therapeutic efficacy of DOXO-MBs. The xenograft cancer model may not reflect the real situation of chemoembolism. But based on our design, DOXO-MBs were supposed to release DOXO to surrounding tumor tissue and induce cellular death. So we performed sub-tumoral injection of DOXO-MBs and compared the therapeutic efficacy of DOXO-MBs with conventional DOXO intravenous (I.V.) injection.

Female athymic nude mice were purchased from Orient Bio Co. (Seoul, Korea). And Green fluorescence protein (GFP)-tagged Hep3B cell line was developed in our lab for the xenograft. Characterization of Hep3B-GFB cells (tumorigenicity, green-fluorescence, cancer drug susceptibility and etc.) for the experiments were fully performed at the time of transfection. $IC_{50}$ of doxorubicin for Hep3B-GFB cells and Hep3B cells was in the same range. Mycoplasma/PPLO testing is done routinely. Passage number of cell lines is precisely controlled. Generally cell lines with passage number over #30 are excluded from the experiments. Green fluorescence protein (GFP)-tagged Hep3B cell line, cultured in DMEM (Gibco®, Thermo Fisher Scientific Inc., Waltham, MA) containing 10% FBS (Gibco®, Thermo Fisher Scientific Inc., Waltham, MA) and 1% antibiotics, was used for the antitumor study. GFP-tagged Hep3B cells were suspended in 100 μl DMEM (without serum) and

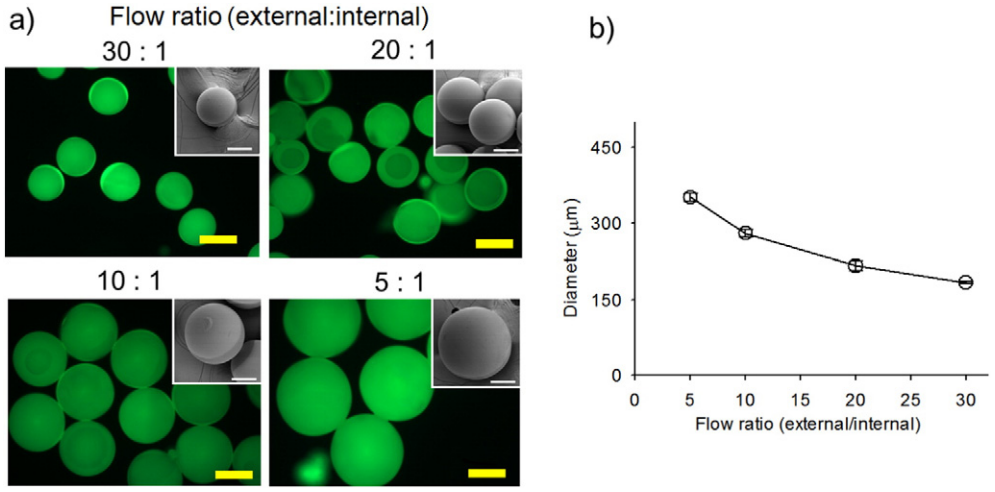


**Fig. 3.** (a) Microscopic observation of FITC-loaded albumin MBs fabricated with different flow ratios (outer solution flow rate: inner solution flow rate). White and yellow bar represent 150 μm and 200 μm in length, respectively. (b) Particle size substantially decreased as the outer solution flow increased. Error bars indicate the standard error of the mean (SEM) for 3 batches of observation.

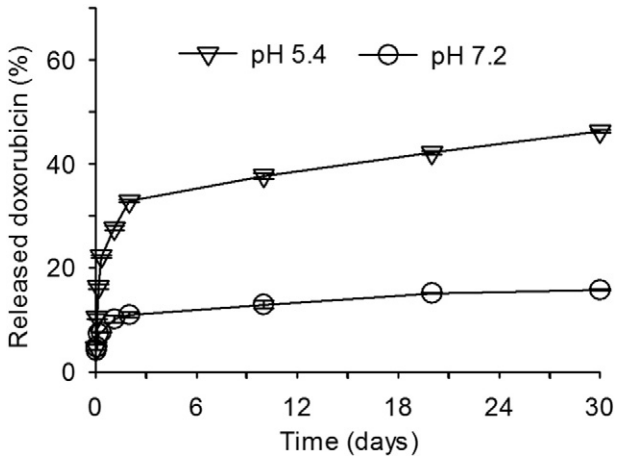


**Fig. 4.** DOXO release profile from DOXO-MBs in pH 5.4 and 7.2 buffers. Error bars indicate the standard error of the mean (SEM) for N = 4.

inoculated into subcutaneous regions of the backs of nude mice (7 to 8 weeks old) under anesthesia. The injected cell numbers varied as $1 \times 10^6$ and $2 \times 10^6$ cells/mouse. Mice were grouped by the injected cell numbers and monitored at least twice a week for evidence of tumor development by quantification of tumor size. Clinically TACE is performed on large hepatic tumor. So our antitumor study was performed when the tumor size grew up to approximately 400 $mm^3$ ($1 \times 10^6$ cells/mouse group) and 600 $mm^3$ ($2 \times 10^6$ cells/mouse group). Tumor size was determined by Vernier caliper measurements and tumor volume was calculated using [length × (width × width) / 2]. In the control groups, the mice were injected with 3 mg/kg DOXO solution via tail vein. In the treatment group, 0.2 ml (tapped volume) of DOXO-MBs containing 3 mg of DOXO were subtumorally inserted after surgical opening of the tumor. After one week, the necrosis of the tumor was observed as purple color, live tumor cells as green and DOXO-MBs in red in an in vivo imaging system. Changes in the tumor size and the body weight of mice were observed for 14 days.

### 2.7. Statistical analysis

All data were presented as the mean ± standard error (SEM) or the mean ± standard deviation (STDEV). The statistical significance between the groups was determined by using the Student's *t*-test. It was considered significant when p values were less than 0.05 or 0.01.

## 3. Results and discussion

### 3.1. Preparation and characterization of DOXO-MBs

DOXO-MBs were prepared using a capillary microfluidic device (Fig. 1). In this experiment, we observed that HSA-DOXO emulsion was generated as droplets as the focused fluid flowed through a constricted section of the capillary tube. The solidification of the w/o emulsions formed by chemical crosslinking reaction of glutaraldehyde with HSA was confirmed, and the morphology of the prepared microbeads was observed by optical microscopy and SEM (Figs. 1c and 2a). Typically, albumin microspheres were fabricated based on w/o emulsion method, and crosslinking agents, mainly aldehydes, were added during the emulsification. But albumin microspheres acquired by this method showed heterogeneous characteristics, i.e., size and morphology. Recovery was also inconsistent by batches.

Intra-arterial embolic particles should have homogeneous size to help particles localize on the arterial bed in predictable ways and to efficiently block the blood supply to the malignant region. In this study, we precisely controlled the size of microbeads by employing the capillary micro fluidic system, and proved that capillary microfluidics is a very attractive method for making homogeneous embolic particles. Reproducible and precise control of particle size, and uniform, high drug loading are cardinal benefits of capillary microfluidics [26]. Fig. 3 shows that the microbeads exhibit a uniform spherical shape with a narrow size distribution. The acquired particles had 183.2 ± 2.2 μm of

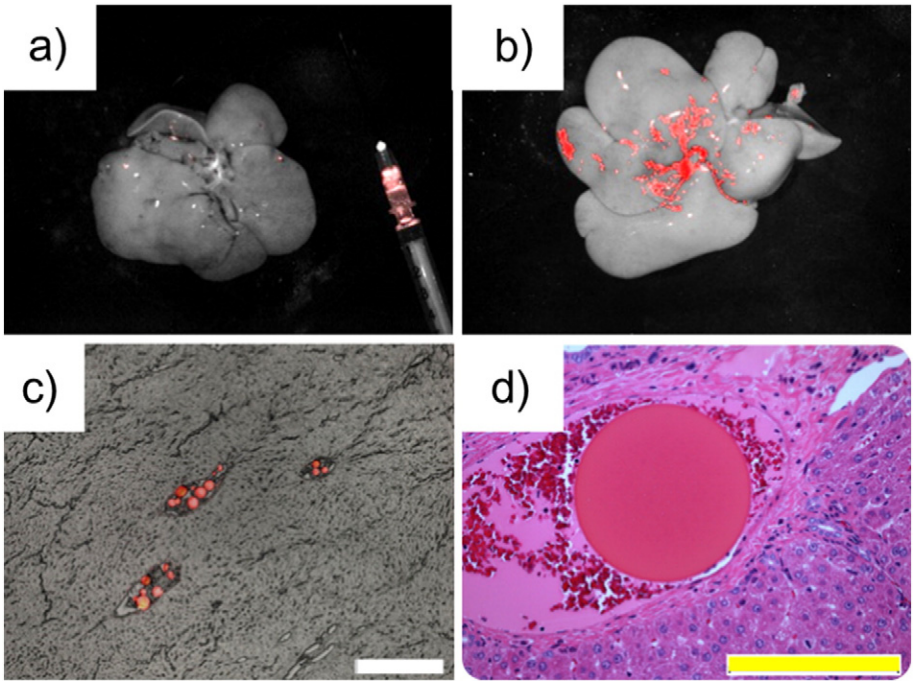


**Fig. 5.** Intrahepatic portal vein injection of DOXO-MBs. (a) and (b) Fluorescence images of whole liver (a) before and (b) after injection of DOXO-MBs. (c) and (d) Embolization of hepatic vessels after injection of DOXO-MBs. Hepatic lobes were immediately recovered after the injection and processed for microscopic observation. White and yellow scale bars represent 500 μm and 100 μm in length, respectively.

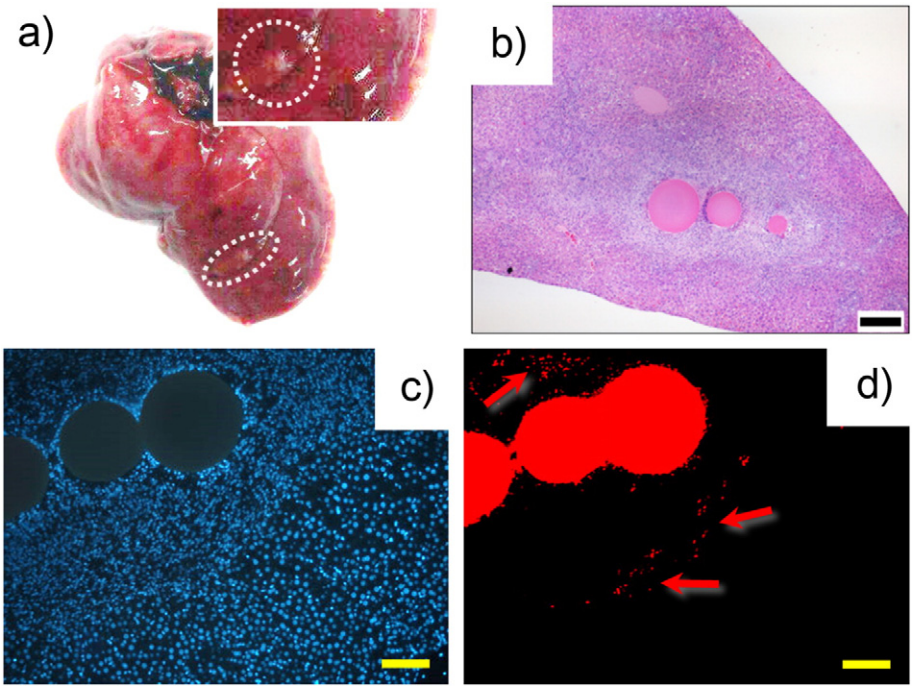


**Fig. 6.** Liver recovered at 24 days after portal vein injection of DOXO-MBs. (a) Whole liver image with some spotted pale ischemic area (white circular area). (b) H&E staining of hepatic lobe. DOXO-MBs located on the middle of hepatic lobe. Black scale bar represents 200 μm in length. (c) DAPI staining of hepatic lobe. DAPI staining suggested the morphological change of nucleus of cells and tissue surrounding the DOX-MBs. (d) Fluorescence microscopic observation of hepatic lobe and DOXO-MBs. Arrows indicate the released-DOXO from DOXO-MBs distributed to surrounding tissue (red fluorescence). Yellow scale bars represent 100 μm in length.

mean particle size at the highest flow ratio of external to internal solution (30:1), and the size subsequently increased to 351.5 ± 7.9 μm at the flow ratio of 5:1. The size of microbeads is very critical for successful embolization of hepatic tumor in clinical treatments. Smaller particles possibly stick into deep side of tumor legion, efficiently block the blood supply and release DOXO. But if the size of

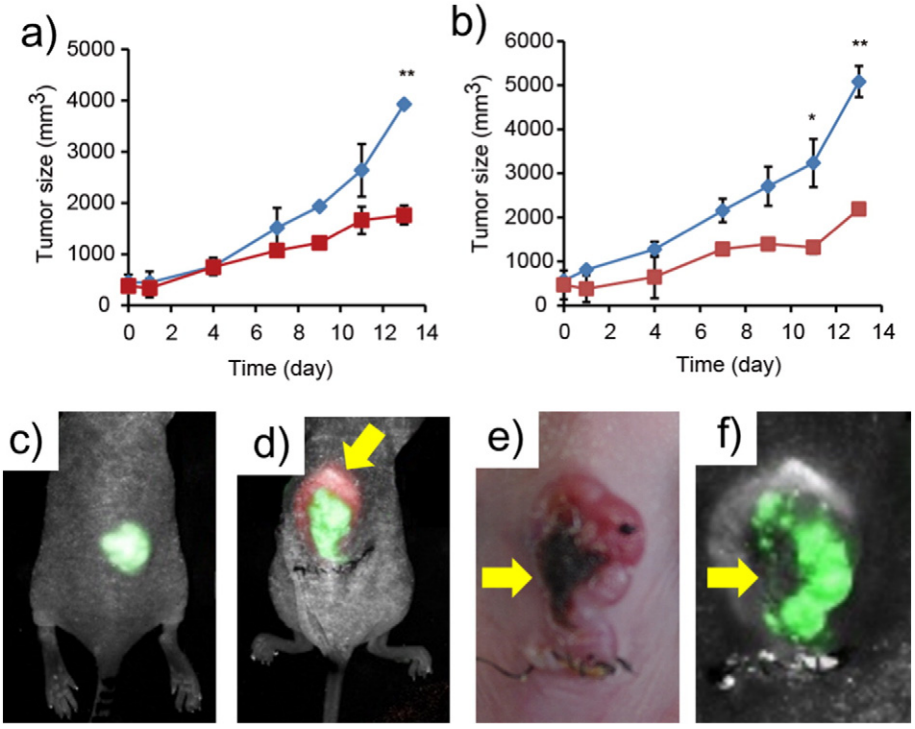


**Fig. 7.** In vivo xenograft tumor growth inhibition study. (a) and (b) Tumor growth inhibition of DOXO-MBs in comparison with DOXO I.V. injection. Study started against different size of tumor, (a) 400 mm$^3$ and (b) 600 mm$^3$, respectively. Error bars indicate the standard error of the mean (SEM) for N = 6. Student's *t*-test was performed, *p < 0.05 **p < 0.01. (c) Subcutaneous xenograft of GFP-tagged Hep3B (green fluorescence). (d) Subtumoral inoculation of DOXO-MBs (red fluorescence). (e) and (f) Locally induced tumor-necrosis after subtumoral inoculation of DOXO-MBs. Green fluorescence represents viable tumor area and the arrows indicate necrotic area induced by DOXO-MBs.

particles is much smaller than the diameter of target tumor vessel, the particles bypass the tumor lesion and distribute to non-targeted organs, such as the lung and biliary tract. On the other hand, large particles tend to clog the common hepatic artery or catheter before accessing the tumor legion.

We also observed the cross-sectioned DOXO-MBs on a SEM, which proved solid core formation of DOXO-MBs (Fig. 2b and c). DOXO content was around 9.7 ± 1.5 mg/g.

### 3.2. In vitro dissolution profile of DOXO

The dissolution profile of DOXO from the DOXO-MBs at pH 7.2 and 5.4 buffer solution is shown in Fig. 4. Drug release from albumin microbeads is usually characterized by a burst release phase followed by a slow release phase. The initial burst release during 24 h was due to drug release from the surface of the microbeads. The initial burst release from the microbeads was approximately 10% of the total drug. The cumulative dissolved amount of DOXO from DOXO-MBs was about 16% over the course of 30 days at pH 7.2. The low dissolution rate during the slow release phase may be explained by degradation and drug diffusion rate of the microbeads. The crosslinking extent of albumin microbeads plays a pivotal role in the drug release from the albumin microbeads [27]. These results indicate that the release profile of DOXO-MBs shows adequate fit to a spherical microbeads model (Fig. 4).

### 3.3. Embolization of rat hepatic vessel and DOXO release

Intrahepatic distribution of the administered DOXO-MBs across the portal vein was studied in Sprague–Dawley rats as an animal model. In this study, we selected rats for histological study. Mouse portal-vein is too small for the injection of DOXO-MBs in size of 200 μm. We also tried DOXO-MBs around 100 μm in size for the injection. And every time we found mouse hepatic vessel was clogged at the injection point. So we moved to the rat model for the study. We injected 100 μm size of the DOXO-MBs which is suitable to pass through the hepatic vessel. Fig. 5a and b shows that the DOXO-MBs were distributed along the hepatic blood vessel and spotted all over the liver. We found particles mainly localized in the central part of liver. A study using a larger animal such as micro-pigs might allow more precise size-dependent localization. H&E staining (Fig. 5c and d) clearly shows the intravascular presence of microbeads in the liver. Thus, the microbeads could be used effectively in embolization therapy to block the blood vessels that supply nutrients to the tumor cells.

Tissue distribution of the DOXO released from DOXO-MBs was observed in the recovered liver at 24 days after the portal vein injection. Fig. 6a, an image of the recovered whole liver, shows DOXO-MBs accumulated in the terminal hepatic lobe. H&E staining and DAPI staining of the hepatic lobe (Fig. 6b and c) shows DOXO-MBs induced deformation of cellular structure surrounding tissue. Based on the fluoroscopic observation (Fig. 6d), we also assumed DOXO released from DOXO-MBs and distributed surrounding hepatic tissue, and the distribution depth was approximately 150–200 μm. And this result coincided exactly with H&E and DAPI staining.

### 3.4. In vivo antitumor efficacy

In vivo antitumor study was performed using a xenograft tumor mouse model to determine whether DOXO-MBs treatment leads to controlled drug delivery and tumor regression of established tumor growth in tumor-bearing mice. In advance, we observed the cytotoxicity of blank microbeads carrier on Chang liver cell lines (see Supplemental data). Figure S1 shows that albumin microbeads did not affect the cell viability, and we assured that albumin microbeads might not induce the tissue toxicity by itself.

For the study, tumors were generated in nude mice by subcutaneous injection of different numbers of GFP-tagged Hep3B cells. The DOXO-MBs containing 3 mg of DOXO were placed intratumorally using a surgical procedure. Whole body images of the HSA-DOXO implanted mice were collected on day 0 and 7 using the Maestro in vivo imaging system. Fig. 7a and b shows DOXO-MBs displayed superior antitumor efficacy compared to control mice (I.V. injection). Fig. 7e and f shows the partial necrotic lesion of the tumor mass. During the experiment we didn't observe any weight change of mouse in each group (see Supplemental figure S2). The in vivo study demonstrated that the DOXO-MBs induce high necrosis to the tumor cells and exhibited potential antitumor effect in the tumor models. Thus, HSA-DOXO microspheres could be an effective drug delivery system for embolization therapy of HCC.

## 4. Conclusions

In summary, DOXO-MBs were successfully prepared using capillary flow focusing method for TACE delivery of DOXO. In vitro release studies of DOXO-MBs proved that DOXO released in controlled manner over a month. Intrahepatic injection study and the antitumor study showed that DOXO-MBs worked as a target-specific carrier and subsequently superior in antitumor effect than I.V. injection of DOXO. Hence, DOXO-MBs could be a good candidate for TACE procedure in the treatment of HCC.

## Acknowledgments

This work was supported by Basic Science Research Program through the National Research Foundation of Korea (NRF) funded by the Ministry of Science, ICT and Future Planning (2014R1A2A2A04006562) and partly supported by Inha University Research Grant (52853-01).

## Appendix A. Supplementary data

Supplementary data to this article can be found online at http://dx.doi.org/10.1016/j.msec.2016.01.073.

## References

[1] A. Jemal, F. Bray, M.M. Center, J. Ferlay, E. Ward, D. Forman, CA Cancer J. Clin. 61 (2011) 69–90.
[2] L.R. Roberts, N. Engl. J. Med. 359 (2008) 420–422.
[3] A.M. Di Bisceglie, R.L. Carithers Jr., G.J. Gores, Hepatology 28 (1998) 1161–1165.
[4] H. Tanaka, S. Kubo, T. Tsukamoto, T. Shuto, S. Takemura, T. Yamamoto, T. Okuda, A. Kanazawa, K. Hirohashi, Transplant. Proc. 37 (2005) 1254–1256.
[5] S. Yamamoto, Y. Sato, T. Takeishi, K. Hirano, T. Kobayashi, T. Watanabe, K. Hatakeyama, Hepato-Gastroenterology 52 (2005) 1083–1086.
[6] J. Kota, R.R. Chivukula, K.A. O'Donnell, E.A. Wentzel, C.L. Montgomery, H.W. Hwang, T.C. Chang, P. Vivekanandan, M. Torbenson, K.R. Clark, J.R. Mendell, J.T. Mendell, Cell 137 (2009) 1005–1017.
[7] J.M. Llovet, M.I. Real, X. Montana, R. Planas, S. Coll, J. Aponte, C. Ayuso, M. Sala, J. Muchart, R. Sola, J. Rodes, J. Bruix, G. Barcelona, Liver cancer, Lancet 359 (2002) 1734–1739.
[8] J.M. Llovet, S. Ricci, V. Mazzaferro, P. Hilgard, E. Gane, J.F. Blanc, A.C. de Oliveira, A. Santoro, J.L. Raoul, A. Forner, M. Schwartz, C. Porta, S. Zeuzem, L. Bolondi, T.F. Greten, P.R. Galle, J.F. Seitz, I. Borbath, D. Haussinger, T. Giannaris, M. Shan, M. Moscovici, D. Voliotis, J. Bruix, S.I.S. Group, N. Engl. J. Med. 359 (2008) 378–390.
[9] S.A. Rosenberg, J.C. Yang, N.P. Restifo, Nat. Med. 10 (2004) 909–915.
[10] J. Wulf, M. Guckenberger, U. Haedinger, U. Oppitz, G. Mueller, K. Baier, M. Flentje, Acta Oncol. 45 (2006) 838–847.
[11] R.J. Lewandowski, J.F. Geschwind, E. Liapi, R. Salem, Radiology 259 (2011) 641–657.
[12] F. Meric, Y.Z. Patt, S.A. Curley, J. Chase, M.S. Roh, J.N. Vauthey, L.M. Ellis, Ann. Surg. Oncol. 7 (2000) 490–495.
[13] K. Nakakuma, S. Tashiro, T. Hiraoka, K. Uemura, T. Konno, Y. Miyauchi, I. Yokoyama, Cancer 52 (1983) 2193–2200.
[14] P.J. Johnson, C. Kalayci, N. Dobbs, N. Raby, E.M. Metivier, L. Summers, P. Harper, R. Williams, J. Hepatol. 13 (1991) 120–127.
[15] J. Kritzinger, D. Klass, S. Ho, H. Lim, A. Buczkowski, E. Yoshida, D. Liu, Clin. Radiol. 68 (2013) 1–15.
[16] J. Kettenbach, A. Stadler, I.V. Katzler, R. Schernthaner, M. Blum, J. Lammer, T. Rand, Cardiovasc. Intervent. Radiol. 31 (2008) 468–476.
[17] R. Martin, D. Geller, J. Espat, D. Kooby, M. Sellars, R. Goldstein, D. Imagawa, C. Scoggins, Hepato-Gastroenterology 59 (2012) 255–260.
[18] A.L. Lewis, M.V. Gonzalez, S.W. Leppard, J.E. Brown, P.W. Stratford, G.J. Phillips, A.W. Lloyd, J. Mater. Sci. Mater. Med. 18 (2007) 1691–1699.

[19] D. Carugo, L. Capretto, S. Willis, A.L. Lewis, D. Grey, M. Hill, X. Zhang, Biomed. Microdevices 14 (2012) 153–163.
[20] A.R. Abate, J. Thiele, D.A. Weitz, Lab Chip 11 (2011) 253–258.
[21] C.H. Yang, K. Huang, P. Lin, Y. Lin, Sensors Actuators B Chem. 124 (2007) 510–516.
[22] C.H. Yang, K.S. Huang, J.Y. Chang, Biomed. Microdevices 9 (2007) 253–259.
[23] H. Zhang, X.J. Ju, R. Xie, C.J. Cheng, P.W. Ren, L.Y. Chu, J. Colloid Interface Sci. 336 (2009) 235–243.
[24] P.W. Ren, X.J. Ju, R. Xie, L.Y. Chu, J. Colloid Interface Sci. 343 (2010) 392–395.
[25] S. Amatya, E.J. Park, J.H. Park, J. Kim, E. Seol, H. Lee, H. Choi, Y. Shin, D.H. Na, J. Pharm. Innov. 43 (2013) 259–266.
[26] S. Freiberg, X.X. Zhu, Int. J. Pharm. 282 (2004) 1–18.
[27] W. Chuo, T. Tsai, S. Hsu, T. Cham, Int. J. Pharm. 144 (1996) 241–245.